Assessing climate change impacts on the near-term stability of the wind energy resource over the United States

S. C. Pryor[1] and R. J. Barthelmie

Atmospheric Science Program, College of Arts and Sciences and the Center for Research in Environmental Science, Indiana University, 702 North Walnut Grove, Bloomington, IN 47405

Edited by M. Granger Morgan, Carnegie Mellon University, Pittsburgh, PA, and approved April 7, 2011 (received for review December 22, 2010)

The energy sector comprises approximately two-thirds of global total greenhouse gas emissions. For this and other reasons, renewable energy resources including wind power are being increasingly harnessed to provide electricity generation potential with negligible emissions of carbon dioxide. The wind energy resource is naturally a function of the climate system because the "fuel" is the incident wind speed and thus is determined by the atmospheric circulation. Some recent articles have reported historical declines in measured near-surface wind speeds, leading some to question the continued viability of the wind energy industry. Here we briefly articulate the challenges inherent in accurately quantifying and attributing historical tendencies and making robust projections of likely future wind resources. We then analyze simulations from the current generation of regional climate models and show, at least for the next 50 years, the wind resource in the regions of greatest wind energy penetration will not move beyond the historical envelope of variability. Thus this work suggests that the wind energy industry can, and will, continue to make a contribution to electricity provision in these regions for at least the next several decades.

uncertainty | wind energy density | internal climate variability | model evaluation | temporal trends

The energy sector comprises approximately two-thirds of global total greenhouse gas emissions and hence has been a focus for climate change mitigation efforts (1). Accordingly, renewable energy resources, including wind power, are being increasingly harnessed to provide virtually greenhouse gas emission-free sources of electricity. The global wind energy resource greatly exceeds current total global energy demand (2). Accordingly, a total of 47 GW of new wind energy electricity generation capacity was added worldwide during 2007 and 2008 (3), which accounted for over 10% of all new power generation capacity. New wind projects installed in the United States over the last five years have more than doubled wind-derived electricity generation capacity (2) to over 40 GW by the end of 2010 (4). Further expansion of the generation capacity is expected, and the 2008 US Department of Energy report *20% Wind by 2030* (5) proposes that by 2030, 20% of US electricity supply could derive from wind turbines.

The wind energy resource is dictated by the incident wind speed and thus is determined by the atmospheric circulation. If there are substantial changes in the near-surface atmospheric flow and storm climates in a greenhouse-gas-warmed world, wind energy, or at least the spatial manifestations thereof, may be affected. Changes in measured near-surface (typically approximately 10 m agl) wind speeds over the last 30 years have been reported (e.g., 6, 7). However, assessing causality for these trends has proved difficult. Key challenges to understanding how climate nonstationarity has, or may, influence the spatial and temporal distribution of near-surface winds and the wind energy resource include:

i. The potentially harnessable "power in the wind" (energy density) scales with the cube of wind speed. Further, electricity generated by a wind turbine is a nonlinear function of the incident wind speed. The power curve for a given turbine describes the relationship between hub-height wind speed and electrical power produced and typically shows a tilted "S" shape—with zero electrical power below "cut-in" wind speeds (typically approximately 4 $m\,s^{-1}$), rapidly increasing to the rated power at wind speeds approximately 15 $m\,s^{-1}$, and then electrical power output remains constant until the "cut-out" wind speed (typically approximately 25 $m\,s^{-1}$). Because hub-height wind speeds above 25 $m\,s^{-1}$ are uncommon in most locations where wind turbines are deployed, power production from wind turbines is dominated by the upper percentiles of the wind speed probability distribution (8). Hence, there is a need for accurate data pertaining to metrics of the wind climate beyond the central tendency, and trends in annual mean wind speeds have little bearing on the viability of wind energy.

ii. There is large inherent variability in the wind climate in many locations at a range of time scales from minutes to decades (8), with the latter being linked to large-scale inherent (natural) climate modes of variability. Metrics of the El Niño Southern Oscillation, Pacific-North American pattern, and the North Atlantic Oscillation all significantly influence the interannual variability of the North American wind climate (9, 10). These internal climate modes may manifest as decadal (or longer) temporal trends in storm and wind climates, which could erroneously be interpreted as being associated with anthropogenic forcing of climate in the absence of detailed, robust, long-term wind speed records (11). How such climate modes may change as the climate evolves remains uncertain (12), which further confounds extrapolation of historical tendencies.

iii. There is a relative paucity of long-term records of near-surface wind speeds, which—coupled with reporting, instrumentation and siting inconsistencies (6), and the highly uneven spatial coverage of surface observing stations (7)—can confound accurate assessment of the presence or absence of temporal trends and dynamical causes thereof. Local land-cover change in the proximity of observational sites and resulting increases of surface roughness, and thus frictional retardation of wind very close to the surface, has been proposed as a primary cause for some recent declines in 10-m wind speeds (7). The influence of such changes declines rapidly with height above the

ENVIRONMENTAL SCIENCES

SUSTAINABILITY SCIENCE

Author contributions: S.C.P. and R.J.B. designed research; S.C.P. and R.J.B. performed research; S.C.P. analyzed data; and S.C.P. and R.J.B. wrote the paper.

The authors declare no conflict of interest.

This article is a PNAS Direct Submission.

[1]To whom correspondence may be addressed. E-mail: spryor@indiana.edu.

This article contains supporting information online at www.pnas.org/lookup/suppl/doi:10.1073/pnas.1019388108/-/DCSupplemental.

surface and may explain the discrepancies between observational and reanalysis datasets (6), because wind speeds in reanalysis datasets are determined primarily by pressure gradients that are insensitive to surface roughness.

For these and other reasons, temporal trends in observed historical wind speed time series should not be interpreted as evidence for likely future tendencies or states, or to make inferences regarding the viability of wind energy now or in the future.

The current generation of coupled atmosphere-ocean general circulation models (AOGCMs) are applied on spatial scales (approximately $2 \times 2°$, or approximately 200×200 km) inappropriate to accurate characterization of wind climates (13). However, tools have been developed to extract higher resolution wind climate projections from coupled AOGCMs. One such tool, the regional climate model (RCM), is increasingly skillful in simulating wind speeds (14). Thus, here we use output from RCM simulations conducted under the North American Regional Climate Change Assessment Program (NARCCAP) (15) to investigate possible changes in the US wind energy resource in the near- to medium-term (i.e., to the middle of the current century). In all cases the RCM simulations were conducted at a grid resolution of approximately $0.44 \times 0.44°$ (approximately 50×50 km), and the wind speeds output from the models were archived at a 3 hourly interval. The future time period (2041–2062) used herein is selected to represent a temporal window that encompasses the possibility of a discernible climate change signal but for which both current and planned wind farms will still be within their operational lifetimes. To evaluate the RCM skill in reproducing the magnitude and spatial variability of the current wind resource over the United States, RCM-derived wind speeds are extrapolated from 10-m height to 50 m, and the resulting wind energy densities are compared with wind power resource estimates from the National Renewable Energy Laboratory (NREL).

Climate projections for risk, vulnerability, and impact assessments should incorporate assessment of projection uncertainty (16). Thus herein we analyze output from a suite of model simulations and apply statistical tools to quantify at least part of the uncertainty in developing spatially discretized projections of the wind resource. We analyze simulations from RCMs nested within lateral boundary conditions from three AOGCMs and one observationally derived dataset (the NCEP-DoE reanalysis) (17), to examine the sensitivity of wind energy density estimates that derives from the model used to provide information to the RCM about conditions outside the RCM model domain. Further we compare and contrast the wind energy fields and climate change signal that derives from variations in the RCM used to conduct the simulations. The future simulations are used to infer a climate change signal in the wind energy resource over the contiguous United States via comparison with wind energy density derived from simulations for a historical period of 1979–2000. Simulations of the future period (2041–2062) are conducted assuming a relatively high greenhouse gas emission scenario and thus climate change forcing (SRES A2) (18). This emission scenario is at the higher end of those considered by the Intergovernmental Panel on Climate Change. It equates to global greenhouse gas emissions of approximately 80 Gt CO_2-eq per year (twice the rate in 2000) by approximately 2055, but given the future period considered is relatively near-term, variations in climate forcing between the different emission scenarios is rather modest (19). Thus, results presented herein are likely representative of a broad suite of possible future greenhouse gas emissions and atmospheric concentrations.

Results

Spatial patterns of average annual mean energy density over the contiguous United States for the historical period (1979–2000) from the four RCM–AOGCM combinations show a high degree of qualitative similarity (Fig. 1). There are differences in the wind energy density estimates from RegCM3 in the three different sets of lateral boundary conditions (Fig. 1), which indicates the key importance of the AOGCM in determining the storm climate and thus wind climate in RCMs (14). However, wind energy density at 10 m from the three RegCM3 RCM simulations (nested in NCEP reanalysis, GFDL and CGCM3) of the current climate show greater spatial coherence than the simulations from the two RCMs nested in CGCM3 (RegCM3 vs. CRCM), indicating the RCM wind climate is not solely a product of the nesting AOGCM. This is further emphasized by the differences in the wind energy resource particularly within the central plains and western United States in simulations of the historical period derived using the three RCMs nested within the NCEP-DoE reanalysis dataset (Fig. S1). These comparisons thus indicate the value of using multimodel simulations or "ensembles" in developing wind resource assessments and climate change projections.

Although the absolute magnitudes of wind energy density show considerable discrepancies between the RCM–AOGCM couplings, comparison with the NREL resource assessments for a

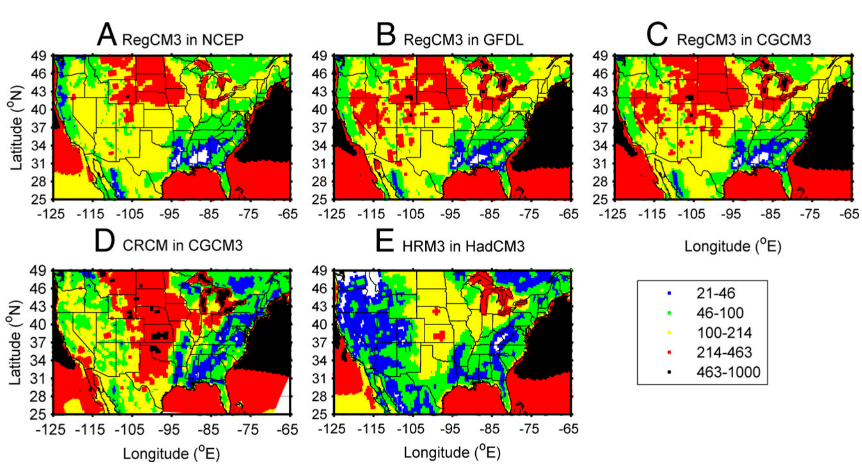

Fig. 1. Mean energy density (in W m^{-2}) for 1979–2000 at a height of 10 m above the surface computed using output from RCM simulations with Regional Climate Model 3 (RegCM3), Canadian Regional Climate Model (CRCM), and Third Generation Hadley Centre Regional Climate Model (HRM3). The different frames show the RCM–AOGCM model chains. The AOGCM abbreviations are Geophysical Fluid Dynamics Laboratory model (CM2.1) (GFDL), Canadian model third generation (CGCM3), third generation Hadley Centre model (HadCM3). *A* shows an example of the wind energy density from the RegCM3 simulation using observed lateral boundary conditions (as specified by the NCEP–DoE reanalysis dataset). Grid cells that are shown in white have an energy density below 21 Wm^{-2}, or in the case of the CRCM–CGCM3 simulation, lie beyond the boundaries of valid RCM output. Note the scale used to depict the wind energy density is logarithmic.

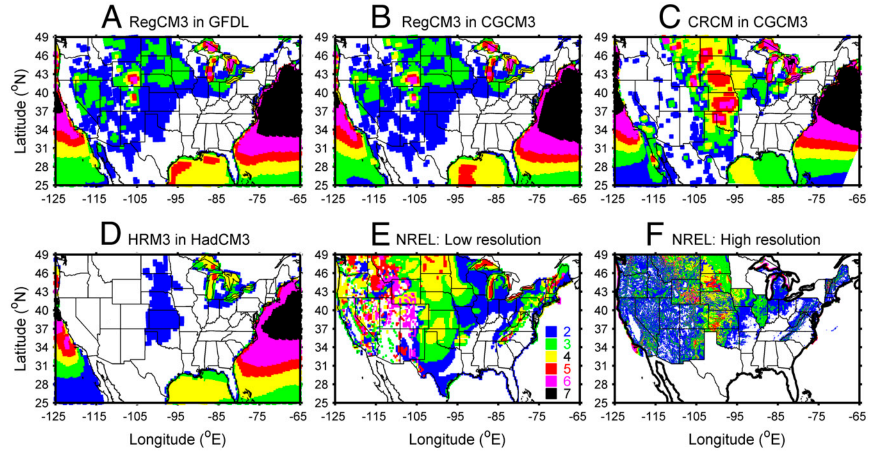

Fig. 2. The wind resource at 50 m in wind power classes: 2, "marginal," wind energy density = 200–300 $W m^{-2}$; 3, "fair," 300–400 $W m^{-2}$; 4, "good," 400–500 $W m^{-2}$; 5, "excellent," 500–600 $W m^{-2}$; 6, "outstanding," 600–700 $W m^{-2}$; and 8, "superb," 700–800 $W m^{-2}$ (28). *A*–*D* show the RCM simulations for 1979–2000 vertically extrapolated from 10 m to 50 m using the NREL procedure of applying the power law with an exponent of 1/7. *D* and *E* show estimates of the annual average wind resource at 50 m from NREL. Estimates in *D* were derived primarily from observational data (28) and have a spatial resolution of 0.25° of latitude by 0.33° of longitude. Estimates depicted in *E* are derived primarily based on modeling assessments for specific states or regions. The original raster data from which the shape files were derived varied in resolution from 200 m to 1,000 m. States or regions with no shading indicate the data have not been made publicly available.

nominal height of 50 m (Fig. 2 *D* and *E*) indicates some degree of skill in all of the RCM simulations. Simulations from the HRM3–HadCM3 model chain exhibit least skill and are negatively biased relative to the other simulations and the wind power resource estimates from NREL. The agreement with the NREL wind power resource estimates is highest for the simulation with CRCM nested in CGCM3, particularly in the central plains states. The central plains region (Fig. 3) is of particular importance because it has the highest wind energy potential (2), and as of the end of 2010, two-thirds of the total national installed wind power capacity was located in the central plains (CP) and Midwest regions (Fig. S2).

When the wind energy resource computed from simulations of the future period (2041–2062) is compared with historical values (1979–2000), all four model combinations indicate only modest differences in the wind resource (Fig. 3). The maximum fraction of grid cells from any simulation that lie beyond the 95% confidence interval on the mean computed from 1979–2000 (i.e., beyond $\pm 1.96\sigma/\sqrt{n}$) is 25% and derives from the simulation with RegCM3 nested in CGCM3. If a study analyzed only output from this simulation (RegCM3 nested within CGCM3) the inference might be made that the mean wind resource in both the western and eastern United States is projected to be up to 15% lower in the future period (Fig. 3*B*). However, no such inference can, or should, be drawn from simulations with CRCM nested in CGCM3 or HRM3 in HadCM3 (Fig. 3 *C* and *D*). All four simulations indicate fairly stable or slightly increased wind resource magnitudes in the southern CP states of Texas, Oklahoma, and Kansas (Fig. 3), which have over one-quarter of currently installed wind capacity (Fig. S2).

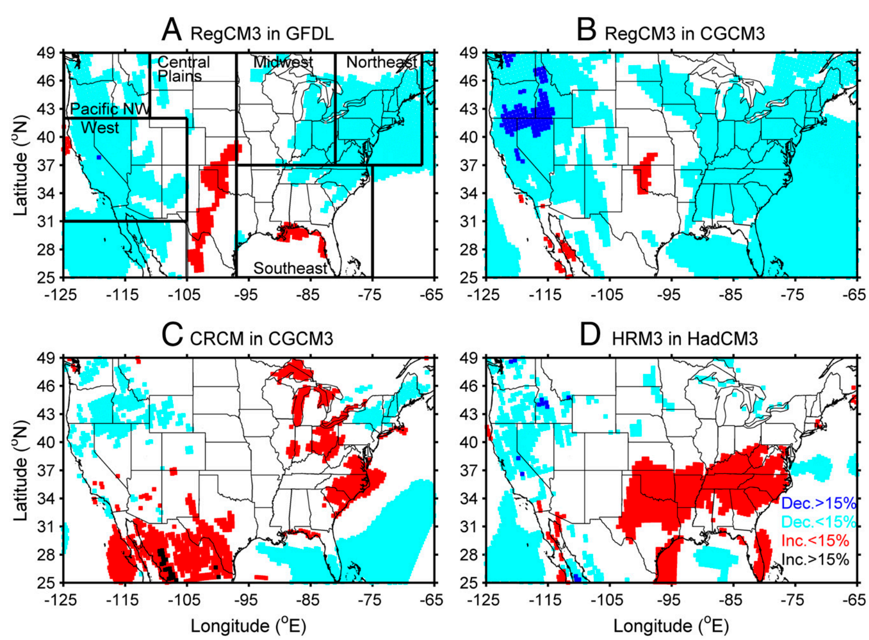

Fig. 3. Difference in the mean wind energy density (in %) for 2041–2062 vs. 1979–2000. *A*–*D* show the different AOGCM–RCM combinations. The sign and magnitude of change is only shown for grid cells where the value for the future period beyond the 95% confidence intervals on the mean value during 1979–2000. The colors depict both the sign and magnitude of the difference using the legend in *D*. The climate regions as derived from the National Assessment and used in Fig. 4 are denoted in *A*.

When the climate change signal from each model combination is contextualized in terms of the wind resource variability during the historical period that derives from the lateral boundary conditions (i.e., the nesting used, Fig. 1) or the RCM applied (Fig. S1), then one can readily infer that the "climate change signal" is of very modest magnitude. In each of the six regions used in the National Climate Assessment (see Fig. 3*A* and ref. 20) for all model combinations, the climate change signal (i.e., difference between the spatial patterns computed for 2041–2062 vs. 1979–2000) is of comparable magnitude to the uncertainty in the historical period due to different model combinations (Fig. 4). The correlation, rmsd, and ratio of spatial standard deviation in the wind energy density patterns for each region are of comparable magnitude in comparisons of spatial fields of energy density from a given RCM nested in either an AOGCM or NCEP, and for the climate change signal derived from simulations by RCMs within a single AOGCM (Fig. 4). Further, the climate change signal is smaller than differences in the wind energy density for the historical period computed using the different RCM–AOGCM combinations (cf. Fig. 1 *A*–*C*). Thus the inference that must be drawn is that there is no statistically significant, or robust, climate change signal in the wind energy density over the contiguous United States projected to the middle of the twenty-first century.

Discussion and Concluding Remarks

Global climate change may change storm dynamics and/or storm tracks and thus the wind resource or the context in which the wind energy industry operates at a given location (8). There has been only very limited research conducted to date, and more research is certainly warranted. Nevertheless, based on an array of RCM simulations, there does not appear to be a consistent climate change signal in the wind resource over the continental United States. Whether the results presented herein are reflective of the true climate change signal or are indicative of model weaknesses cannot yet be definitively asserted. The current formulations and parameterizations used in these RCMs and the application at a 50-km grid spacing precludes treatment of some important phenomena. It is possible that future high-resolution RCM simulations conducted using the next generation of models may exhibit different sensitivity to greenhouse gas forcing (21). However, based on the analysis presented herein and the literature cited, there is no clear tendency in the near- to medium-term for the wind resource over the contiguous United States.

Similar analyses over northern Europe found comparable results. In the near-term (i.e., to the middle of the current century) natural variability exceeds the climate change signal (14). In the longer term, there is some weak evidence for increases in the wind energy resource at least over Scandinavia (14).

Materials and Methods

The energy density in the wind, and hence the power that can potentially be harnessed by wind turbines, scales with the cube of the wind speed at wind turbine hub height:

$$E = \frac{1}{2}\rho U^3, \quad [1]$$

where E is the instantaneous energy density (W m^{-2}), ρ is the air density (kg m^{-3}), and U is the instantaneous wind speed (m s^{-1}).

Herein we use RCM output at a standard height of 10 m above ground as an analogue of the wind speed at wind turbine hub height and compute the annual mean energy density for each RCM simulation and grid cell using Eq. **1**.

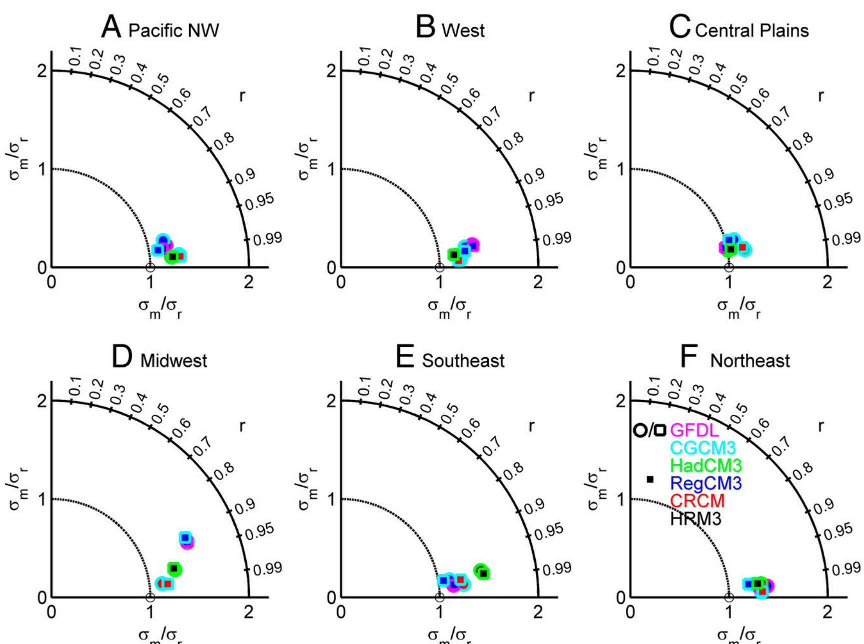

Fig. 4. Taylor diagrams of wind energy density in each of the six regions shown in Fig. 3*A*, (*A*–*F* depict each of the regions) for each RCM simulation. The metrics shown are computed by comparing the spatial patterns of average wind energy density in each region from each simulation. They are the correlation (r), normalized standard deviation (σ_m/σ_r, derived from a given model (subscript m) and a reference simulation [subscript r)], and rmsd of the spatial fields. The comparisons were undertaken for each of the different AOGCM–RCM combinations during the historical period and for the climate change projection period relative to the historical period (i.e., 2041–2062 vs. 1979–2000). For the climate change simulations (denoted by the squares) the comparison is for a given AOGCM–RCM combination. Thus the model field represents 2041–2062, while the reference field is for 1979–2000. For analysis of the importance of lateral boundary conditions (denoted by the circles) the RCM is held constant and the reference field shows simulations nested in NCEP reanalysis, while the model field derives from the specified AOGCM. The color of the outer ring indicates the nesting AOGCM, while the inner portion of the symbol denotes the RCM used. The shape of the outer ring denotes the following: The squares show the climate change signal (i.e., 2041–2062 vs. 1979–2000), while the circles denote the differences in the historical period (1979–2000) due to the lateral boundary (nesting) conditions. In each frame the correlation coefficient (r) is shown by the azimuthal angle; the ratio of the standard deviation in the fields (σ_m/σ_r) is shown by the radial distance from the origin (o, which is located at $r = 1$, $\sigma_m/\sigma_r = 1$, and rmsd = 0), and the rmsd in the fields is shown by the distance from the origin (o).

The RCM simulations analyzed herein were conducted as part of NARCCAP (15). The model experiment was designed to sample multiple RCMs nested in multiple coupled AOGCMs. Herein we use output from three RCMs: regional climate model 3 (RegCM3) (22), Canadian regional climate model (CRCM) (23), and third generation Hadley Centre regional climate model (HRM3) (24). The three AOGCMs used to provide the lateral boundary conditions are Geophysical Fluid Dynamics Laboratory model (GFDL) (CM2.1) (25), Canadian model version 3 (CGCM3) (26), and Hadley Centre model, third generation (HadCM3) (27). Further, a set of numerical experiments in which the RCMs are nested within output from the NCEP-DoE global reanalysis (17) are analyzed to investigate differences in wind energy density during the historical period that derive from using AOGCM output rather than observations (as approximated in the reanalysis dataset). The model combinations analyzed herein represent the entirety of simulations available from the NARCCAP project as of December 2010.

To evaluate the RCM skill in reproducing the magnitude and spatial variability of the current wind resource over the United States, RCM-derived wind speeds are extrapolated from 10-m height to 50 m using the power law with an exponent of 1/7 (i.e., $U_{50} = U_{10} \times (\frac{50}{10})^{1/7}$) following the approach used in developing the Wind Resource Map at NREL (28), and the results are compared with NREL-derived wind power resource estimates.

Differences in the wind resource spatial patterns from different models in the historical period (1979–2000) are used to contextualize the climate change signal derived from simulations of 2041–2062. We present results of climate change projections in the context of the historical period and show percent changes in the mean wind energy density in a given grid cell during the future period if it lies beyond the 95% confidence intervals (CI) on the mean energy density computed for 1979–2000. These CI are computed from the standard error as $CI = \frac{1.96\sigma}{\sqrt{n}}$, where n = sample size (22 years), and σ is the standard deviation of annual mean energy density computed for 1979–2000.

We provide a synthesis of comparisons of the climate change signal with the sensitivity to lateral boundary conditions by comparing the spatial fields of wind energy density for different model periods and combinations. Thus the field of mean wind energy density for a simulation with a given RCM nested in output an AOGCM is compared to a reference field derived from the same RCM nested within data from the NCEP reanalysis product. This comparison quantifies the difference in wind energy density that derives from differences in the lateral boundaries (i.e., the model used to provide information beyond the domain for which the RCM computes atmospheric conditions). This difference is then compared to the climate change signal in wind energy density computed by running a given RCM nested in AOGCM output for the future time period relative to the reference field derived from simulations by that same RCM nested in AOGCM output for the historical period. In each time period and model combination we make comparisons of the spatial patterns of mean wind energy density in geographic regions (see Fig. 3). These regions broadly represent those used in the US National Climate Assessment (20). Key metrics used for this comparison are the correlation coefficient (r) of the fields shown by the azimuthal angle on a Taylor diagram (29), the degree of spatial variability as depicted by the ratio of the standard deviation in the fields (σ_m/σ_r) (shown by the radial distance from the origin, where $\sigma_m/\sigma_r = 1$), and the root mean square difference (rmsd) between the fields (shown by the distance from the origin) (Fig. 4).

ACKNOWLEDGMENTS. Financial support was supplied by the National Science Foundation (NSF) (Grant 1019603), the International Atomic Energy Authority, and the Center for Research in Environmental Science of Indiana University. We wish to thank the North American Regional Climate Change Assessment Program (NARCCAP) for providing the RCM output used in this paper. NARCCAP is funded by the NSF, the US Department of Energy, the National Oceanic and Atmospheric Administration, and the US Environmental Protection Agency Office of Research and Development. The National Renewable Energy Laboratory (NREL) wind power resource estimates were obtained from the GIS data portal developed and operated by NREL (http://www.nrel.gov/gis/data_analysis.html).

1. Sims REH, et al. (2007) Energy supply. *Climate Change 2007: Mitigation. Contribution of Working Group III to the Fourth Assessment Report of the Intergovernmental Panel on Climate Change*, eds B Metz, OR Davidson, PR Bosch, R Dave, and LA Meyer (Cambridge Univ Press, Cambridge, UK), pp 251–322.
2. Lu X, McElroy MB, Kiviluoma J (2009) Global potential for wind-generated electricity. *Proc Natl Acad Sci USA* 106:10933–10938.
3. Musgrove P (2010) *Wind Power* (Cambridge Univ Press, Cambridge, UK).
4. AWEA (2011) *AWEA: US Wind Industry Year-End 2010 Market Report*, Available at http://www.awea.org/learnabout/publications/upload/4Q10_market_outlook_public.pdf.
5. National Renewable Energy Laboratory (2008) *20% Wind Energy by 2030: Increasing Wind Energy's Contribution to US Electricity Supply* (US Department of Energy, Washington, DC).
6. Pryor SC, et al. (2009) Wind speed trends over the contiguous United States. *J Geophys Res* 114:D14105.
7. Vautard R, Cattiaux J, Yiou P, Thepaut JN, Ciais P (2010) Northern hemisphere atmospheric stilling partly attributed to an increase in surface roughness. *Nat Geosci* 3:756–761.
8. Pryor SC, Barthelmie RJ (2010) Climate change impacts on wind energy: A review. *Renew Sust Energy Rev* 14:430–437.
9. Pryor SC, Ledolter J (2010) Addendum to: Wind speed trends over the contiguous USA. *J Geophys Res* 115:D10103.
10. Enloe J, O'Brien JJ, Smith SR (2004) ENSO impacts on peak wind gusts in the United States. *J Clim* 17(8):1728–1737.
11. Barring L, Fortuniak K (2009) Multi-indices analysis of southern Scandinavian storminess 1780–2005 and links to interdeceadal variations in the NW Europe-North Sea region. *Int J Climatol* 29:373–384.
12. Keeley SPE, Collins M, Thorpe AJ (2008) Northern hemisphere winter atmospheric climate: Modes of natural variability and climate change. *Clim Dynam* 31:195–211.
13. Pryor SC, Schoof JT, Barthelmie RJ (2006) Winds of change? Projections of near-surface winds under climate change scenarios. *Geophys Res Lett* 33, 10.1029/2006GL026000.
14. Pryor SC, et al. (2011) Analyses of possible changes in intense and extreme wind speeds over northern Europe under climate change scenarios. *Clim Dynam*, 10.1007/s00382-010-0955-3.
15. Mearns LO, et al. (2009) A regional climate change assessment program for North America. *EOS* 90:311–312.
16. Hawkins E, Sutton R (2009) The potential to narrow uncertainty in regional climate projections. *Bull Am Meteorol Soc* 90:1095–1107.
17. Kanamitsu M, et al. (2002) NCEP-DOE AMIP-II reanalysis (R-2). *Bull Am Meteorol Soc* 83:1631–1643.
18. Nakicenovic N, Swart R, eds. (2000) *Emissions Scenarios* (Cambridge Univ Press, Cambridge, UK) p 570.
19. Solomon S, et al. (2007) *Climate Change 2007: The Physical Science Basis. Contribution of Working Group I to the Fourth Assessment Report of the Intergovernmental Panel on Climate Change* (Cambridge Univ Press, Cambridge, UK) p 996.
20. National Assessment Synthesis Team (2000) *Climate Change Impacts on the United States—Overview Report: The Potential Consequences of Climate Variability and Change* (Cambridge Univ Press, Cambridge, UK), Available from http://www.globalchange.gov/publications/reports/scientific-assessments/us-impacts, p 158.
21. Bengtsson L, Hodges KI, Keenlyside N (2009) Will extratropical storms intensify in a warmer climate? *J Clim* 22:2276–2301.
22. Pal JS, et al. (2007) Regional climate modeling for the developing world—The ICTP RegCM3 and RegCNET. *Bull Am Meteorol Soc* 88:1395–1409.
23. de Elia R, Cote H (2010) Climate and climate change sensitivity to model configuration in the Canadian RCM over North America. *Meteorol Z* 19:325–339.
24. Jones RG, et al. (2004) Generating high resolution climate change scenarios using PRECIS. (Met Office Hadley Centre, Exeter, UK) p 35.
25. Delworth TL, et al. (2006) GFDL's CM2 global coupled climate models—Part 1: Formulation and simulation characteristics. *J Clim* 19:643–674.
26. Scinocca JF, McFarlane NA, Lazare M, Li J, Plummer D (2008) Technical note: The CCCma third generation AGCM and its extension into the middle atmosphere. *Atmos Chem Phys* 8:7055–7074.
27. Pope V, Gallani M, Rowntree P, Stratton R (2000) The impact of new physical parameterizations in the Hadley Center climate model: HadAM3. *Clim Dynam* 16:123–146.
28. Elliott DL, Holladay CG, Barchet WR, Foote HP, Sandusky WF (1986) *Wind Energy Resource Atlas of the United States* (Solar Technical Information Program, US Department of Energy, Washington, DC), p 210, Available at http://rredc.nrel.gov/wind/pubs/atlas/.
29. Taylor KE (2001) Summarizing multiple aspects of model performance in a single diagram. *J Geophys Res* 106:7183–7192.